(Preprint) AAS 17-759

EFFICIENT NRHO TO DRO TRANSFERS IN CISLUNAR SPACE

Gregory Lantoine*

There has been recently a growing interest in cislunar missions, in particular for supporting human deep space exploration. Understanding the dynamical environment between various cislunar orbits is therefore useful. The current study is focused on finding efficient transfer trajectory options between a Near-Rectilinear Halo Orbit (NRHO) and a Distant Retrograde Orbit (DRO) in the Earth-Moon system. A general methodology is introduced to design these transfers in a systematic way, including the use of solar perturbations and lunar flybys. Representative solutions are presented and compared in terms of delta-v and flight time, including a transfer requiring 56 m/s only.

INTRODUCTION

In preparation for the human deep space exploration anticipated in the near future, many options to conduct complex operations in cislunar space are being currently studied by NASA.[1] These mission concepts within the Earth-Moon system often include habitats for testing long-duration space missions, propulsion stages for facilitating transfers to interplanetary destinations, or infrastructures for supporting lunar surface activities. To that end, two cislunar orbit types are especially attractive, both in terms of access from Earth (with a crewed spacecraft), multi-mission staging, or access to other destinations: 1) NRHO orbits, which are a specific subset of the Earth-Moon Halo families with higher stability than the more traditional Halo orbits in the vicinity of the Lagrange points;[2,3] and 2) DRO orbits, which appear to orbit the Moon in a retrograde motion (when viewed in a frame rotating with the Moon) and can be long-term stable.[4] One of the mission concepts that take advantage of these orbits is the recently proposed NASA's Asteroid Redirect Robotic Mission (ARRM).[5,6] The ARRM spacecraft would rendezvous with a 100+ m class near- Earth asteroid and bring back a 20-t boulder back to cislunar space, via low-thrust solar electric propulsion. It turns out that the NRHO and DRO orbits can meet two important objectives of the proposed ARRM concept. First, a NRHO orbit is the preferred location for a subsequent crewed mission to investigate the retrieved boulder. Then, a long-term stable DRO orbit can be used to safely store the boulder indefinitely. Due to the large mass of the boulder, it is crucial to minimize as much as possible the transfer delta-v between the NRHO and DRO orbits to enable a feasible ARRM mission. More generally, many more mission scenarios in cislunar space could also benefit greatly from efficient NRHO to DRO transfers, particularly to increase flexibility and meet conflicting mission objectives. As interest in these orbits is likely to continue to increase, it follows that a systematic methodology to construct efficient transfers between NRHO and DRO orbits is definitely warranted at this point in time.

* Mission Design Engineer, Mission Design and Navigation Section, Jet Propulsion Laboratory, California Institute of Technology, 4800 Oak Grove Dr. Pasadena, CA 91109, gregory.lantoine@jpl.nasa.gov.

However, transfers between these orbits are not readily available in the literature. Because of the inherent multi-body forces in play, transfers between these orbits are challenging to find and optimize. Parish and Parker were able to find low-thrust transfers between DRO and Halo orbits in the vicinity of the Lagrange points, but they are costly (on the order of 300-500 m/s) with transfer times of about 30-60 days.[7] Note that these transfers would be even more expensive for NRHOs since these orbits are more stable than Halo orbits located farther from the Moon. The goal of this paper is therefore to fill the gap in the knowledge of low-DV transfers between NRHO and DRO orbits, and develop a method to facilitate the design of these cheap transfers. The transfers constructed using this method will rely on connecting effectively NRHO departure arcs to DRO insertion arcs, via Earth and solar gravity.

The paper is structured as follows. First, the particular NRHO and DRO orbits considered in this analysis are described. Then, a methodology to generate good initial guesses of transfers in a systematic way is discussed. Next, the optimization strategy to transition these initial guesses in an ephemeris model is presented. Finally, representative solutions are provided.

ORBITS CONSIDERED

The particular NRHO and DRO orbits considered in this paper are discussed below.

NRHO orbit

The first orbit considered in this study is the Near Rectilinear Halo Orbit (NRHO). NRHOs are members of the lunar Halo families with close approaches over one of the lunar poles. Farthest point from the Moon is around ~75,000 km (farther than the Earth-Moon L2 distance). Thus, they appear as large elliptical, inclined orbits in a frame rotating with the Moon. They were discovered in the 80s by continuing Halo families towards the secondary body.[8] These orbits are studied in detail in Reference 2. NRHOs can be classified by the period (typically around 6-8 days), or their periapsis radius with respect to the Moon (typically between 3,000 km and 10,000 km). Since NRHOs favor both access from Earth and polar surface access, they are good staging orbits for space modules or habitats. These orbits are just slightly unstable, requiring less than 10 m/s per year of maintenance.[3]

Several steps are needed to generate these orbits in the ephemeris model. First, the full family of Halo orbits is computed in the ideal Circular Restricted Three-Body (CR3BP) model. Starting from a single converged Halo solution arising from a bifurcation in the Lyapunov orbit family, a continuation method is used to generate solutions throughout the entire Halo family. Only solutions near the Moon are kept to form a NRHO orbit database parametrized by orbit period. A particular NRHO orbit corresponding to a desired period can be extracted to construct an initial guess as a series of patch points. This initial guess is transitioned into an ephemeris force model using the multiple-shooting Level 2 differential corrector.[9]

For cislunar applications, Southern L2 NRHOs are often preferred due to their good coverage of the lunar South Pole.[1] The particular Southern L2 NRHO considered in this paper is a 9:2 resonant NRHO (9 NRHO revs per 2 lunar months) with a period of 6.6 days (3250 km periapsis radius). One of the main advantages of a 9:2 NRHO is a reduced number of eclipses by the Earth.[2] Figure 1 shows this orbit in inertial and synodic frames. Table 1 gives the states of this orbit at a particular epoch.

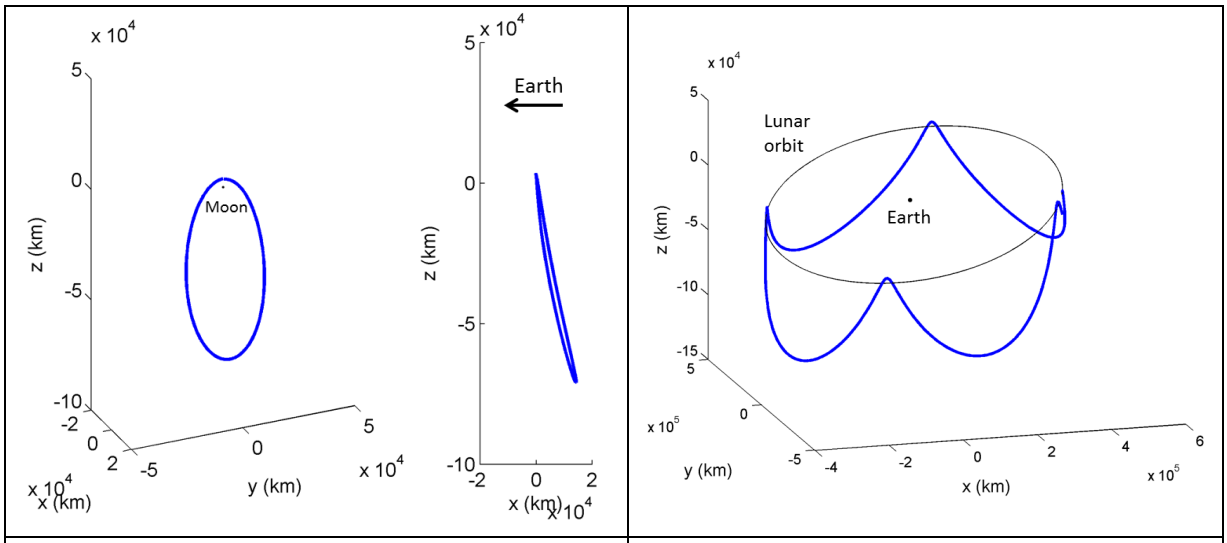

(a) Lunar NRHO in Earth-Moon synodic frame propagated for 1 period

(b) Lunar NRHO in Earth-centered inertial frame propagated for 4 periods

Figure 1. Lunar NRHO considered in this paper.

Table 1. Example of NRHO states in Moon-centered, EMO2000 frame.

Epoch	2026 DEC 15 16:37:21.08285
x (km)	-0.210110371754447e+3
y (km)	0.271395173437642e+3
z (km)	3.522188146738426e+3
vx (km/s)	0.776406224406541
vy (km/s)	1.425639023143207
vz (km/s)	0.023805751325195

DRO orbit

The second orbit considered is a planar Distant Retrograde Orbit (DRO). Planar DROs appear to be elliptical in shape around the Moon in the rotating coordinate system, and lie in the lunar orbital plane. Typically, a DRO can be classified by the minor axis length of the ellipse (along the Earth-Moon line, at the *x*-crossing in the rotating frame) or its orbit period. Contrary to the relatively new NRHOs, DROs have been well characterized in the Circular Restricted Three-Body Problem (CR3BP) by a myriad of authors over the past 50 years, notably Broucke[10] and Henon[11]. It was found that planar DROs are stable well above the Lagrange points. However, perturbing forces (solar gravity in particular) in the full ephemeris model tend to reduce the number of stable DROs.[4] In that context, an interesting member of the DRO family is the 70k-DRO (shown in Figure 2), with a minimum lunar distance of ~70,000 km (i.e. minor axis length of the DRO ellipse) and an orbital period of around 13-14 days. Table 2 gives the states of this orbit at a particular epoch. That orbit was generated using a similar approach as the one described for the NRHO orbits. A family of DROs was initially constructed in the CR3BP, and a Level 2 differential corrector was used to transition the 70k-DRO into a full ephemeris model.

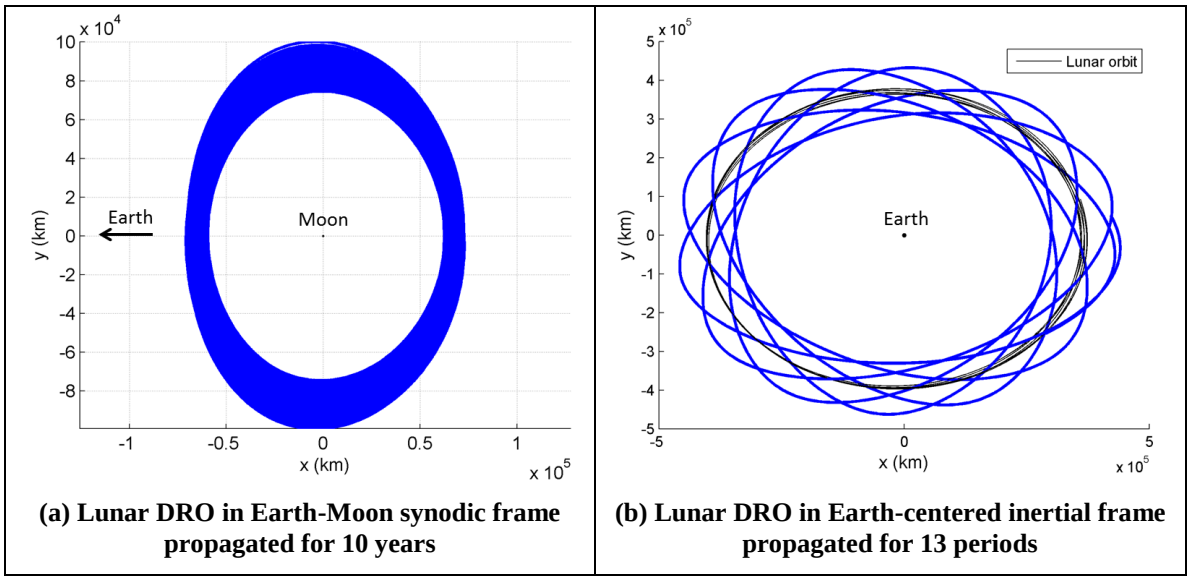

(a) Lunar DRO in Earth-Moon synodic frame propagated for 10 years

(b) Lunar DRO in Earth-centered inertial frame propagated for 13 periods

Figure 2. Lunar DRO considered in this paper.

Table 2. Example of DRO states in Moon-centered, EMO2000 frame. These states are located at the y-crossing in the rotating frame.

Epoch	2025 JAN 29 06:12:58.37833
x (km)	7.006297998479835e+4
y (km)	5.006352175136821e+4
z (km)	0.489708863788025e+4
vx (km/s)	0.060533650318577
vy (km/s)	-0.111443777216460
vz (km/s)	-0.010470486200574

Our stability analysis shows that this orbit is highly stable with more than 150 years of life-time without maintenance. This analysis was performed by propagating ballistically the initial states of the orbit (given in Table 2) using the JPL Planetary Ephemeris DE430 (due to its long time range of validity) with gravitational point masses for the Sun, Earth, and the Moon. The gravitational parameter values used are given in Table 3. To account for navigation errors, this analysis was also expanded to compute the orbit lifetime as a function of position and velocity deviations around the nominal states (still given in Table 2), up to 10 km in position and 10 m/s in velocity. Each perturbed states are ballistically propagated until a significant orbit growth (> 150,000 km from the Moon) or a surface impact is encountered. As shown in Figure 3, position and velocity errors of 10 km and 1 m/s can be accommodated in the orbital plane without losing long-term stability. Larger out-of-plane errors can be also tolerated. These orbit injection error values should be acceptable for most spacecraft around the Moon using standard OD & navigation techniques.[12] Given its long-term stability, this planar DRO is therefore an ideal storage orbit for sample return missions. In addition, the period of this orbit is close to be in 2:1 resonance with the Moon's orbital period, which can provide launch opportunities from Earth every other revolution to access that orbit.

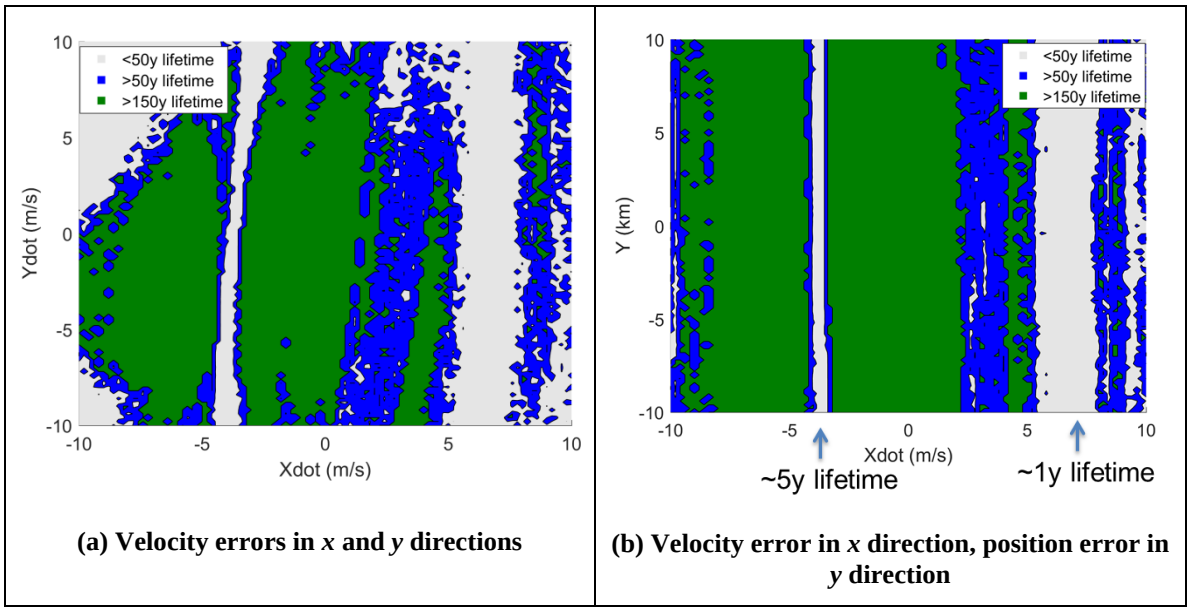

(a) Velocity errors in *x* and *y* directions

(b) Velocity error in *x* direction, position error in *y* direction

Figure 3. Orbit lifetime as a function of position and velocity errors (expressed in Earth-Moon rotating frame). The origin (0,0) corresponds to the nominal DRO orbit states given in Table 2.

Table 3. Gravitational parameters of the Sun, Earth, and Moon.

Parameter	Value
Sun gravitational parameter	1.327124400419400e11 km2/s2
Earth gravitational parameter	3.986592936294783e5 km2/s2
Moon gravitational parameter	4.843941639988467e3 km2/s2

INITIAL GUESS GENERATION

NRHO and DRO orbits are inherently three-body orbits significantly perturbed by the gravity of the Moon and the Earth. As a result, applying standard two-body techniques (such as a Hohmann transfer or a bi-elliptical transfer) to compute transfers between these orbits is not likely to produce satisfactory results. The choice and structure of the initial guess has a strong impact on the quality of the converged solutions. Generally, a gradient-based optimizer is used to solve orbit transfers. Although finding solutions from poor initial guesses is feasible with robust, gradient-based algorithms,[7] the results are more likely to fall into bad local minima. Understanding and exploiting the dynamics involved in a NRHO to DRO transfer is therefore critical to generate a good initial guess and facilitate the design process.

Considering the NRHO and DRO characteristics described in the previous section, it is clear that a NRHO to DRO transfer inherently requires a significant inclination change around the Moon. Inclination changes are expensive, for instance a simple 90-deg plane change starting on a planar DRO at 70,000 km from the Moon would take around 375 m/s using a single maneuver. This high delta-v value suggests that a different strategy should be used. Interestingly, inclination changes are more efficient when performed farther from the orbiting body when the spacecraft velocity is lower. Taking this idea to the extreme, an alternative strategy to perform such transfers would be therefore to take an indirect route by escaping the Moon, performing a small maneuver

at a large distance from the Earth-Moon system, and coming back near the Moon again. Belbruno had a similar strategy to change inclination around the Earth.[13] In this paper, the structure of the initial guess follows that general strategy and is decomposed into three sequential phases (see Figure 4): 1) NRHO departure near the Moon; 2) Transfer leg to come back near the Moon (Moon-to-Moon transfer); 3) DRO insertion near the Moon. The transition between each phase occurs at a given distance from the Moon. The particular radius value chosen is somewhat arbitrary and not critical, nevertheless it is recommended to transition at a distance greater than the two-body lunar sphere of influence radius (~65,000 km[14]) or the three-body lunar sphere of influence radius (~159,200 km[15]) defined in the literature. In this analysis, it was found that transitioning at a distance of ~400,000 km from the Moon was giving satisfactory results. Such a distance encompasses not only the L1 and L2 Lagrange points, but also the L4 and L5 Lagrange points. Nevertheless, the results are not likely to change significantly with slightly different boundary values.

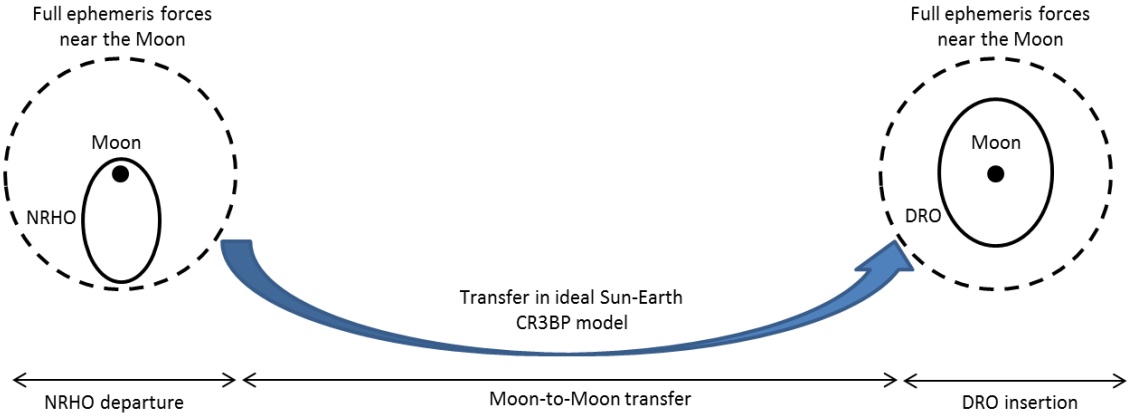

Figure 4. Overall structure and models of the initial guess for efficient NRHO to DRO transfers.

Different set of dynamics are appropriate for each phase. On one hand, near the Moon, full ephemeris forces are considered. In fact, not only NRHO and DRO orbits are strongly shaped by the Earth gravity (they are inherently Earth-Moon three-body orbits after all), but they are also significantly perturbed by the Sun, even when close to the Moon.[4] It follows that accurate initial guesses of trajectories departing from or inserting into these orbits must include gravity forces from the Moon, the Earth and the Sun. In addition, the eccentricity of the Moon plays also a major role in the dynamical environment near these orbits, which explains why ephemeris models are preferable. On the other hand, far from the Moon, lunar gravity becomes negligible on the spacecraft dynamics. Since solar gravitational perturbations are still significant (as well as Earth's gravity of course), the spacecraft motion is then modeled by the circular restricted Sun–Earth three-body problem. For simplicity, the Sun, the Earth and the (massless) Moon are all in circular, coplanar orbits in this model. This basic model is attractive because it is epoch independent.

Overall, this patched model simplifies the initial guess generation by splitting the transfer into three independent phases. Nevertheless, the fundamental dynamics at play between the Earth, Moon and Sun gravitational forces are still preserved. This strategy is based on the same principles as the patched three-body model of Parker,[15] but enables a spacecraft in the near-Moon environment to be affected by all three massive bodies for higher fidelity. The following sub-sections describe in detail the initial guess generation of each phase.

Moon-to-Moon transfer

The first critical building block for a good initial guess is to find a trajectory that leaves the Moon at a small relative velocity (after NRHO departure) and comes back later to the Moon with a similar low relative velocity (for setting up DRO insertion). For conic trajectories, the problem would be simply reduced to finding a solution in resonance with the Moon's orbital period. However, as described above, solar perturbations have to be taken into account. Even assuming simplifying circular and planar assumptions, finding Moon-to-Moon transfers in the Sun-Earth CR3BP is typically challenging and tedious as no closed-form solutions of the three-body problem are known. Fortunately, solutions can be easily found by looking up an existing database of families of Moon-to-Moon transfers in the Sun-Earth CRTBP.[16] Each family corresponds to different number of months between lunar encounters, implied by the order in the alphabet of the uppercase letter in each family name. Note that two lowercase letters 'oi' are added to the family names to reflect the fact that lunar departure naturally occurs on an outbound ('o') trajectory while lunar insertion occurs on an inbound ('i') trajectory at the end. Each 'oi' family can be uniquely defined by a set of four parameters that are illustrated in Figure 5:

- Initial solar phase angle θ_0: angle between Sun-Earth and Earth-Moon lines (see Figure 5) at the start of the transfer (angle between the initial lunar location and the solar direction). This angle is an important parameter as it defines the geometry of the Sun-Earth-Moon system.
- Initial lunar relative velocity $v_{\infty,0}$
- Pump angle α_0 between the v_∞ vector and lunar velocity vector
- Flight time TOF between lunar encounters

Only two parameters, the initial lunar relative velocity $v_{\infty,0}$ and the initial solar phase angle θ_0, need to be specified to retrieve a solution member within each family.

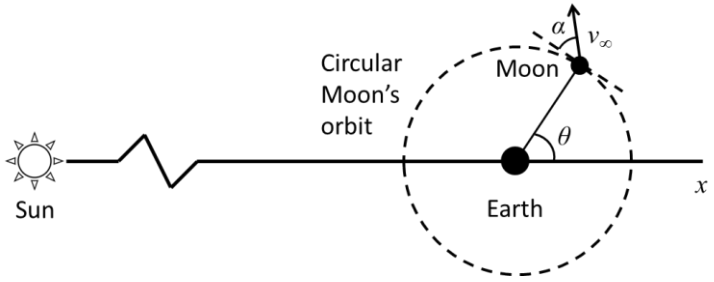

Figure 5. Illustration of the model considered for Moon-to-Moon transfers

Relevant characteristics of the 'oi' families with a small initial lunar relative velocity of 0.4 km/s are given in Figure 6. The small initial lunar relative velocity simulates a low-energy departure from the NRHO orbit. The flight time plot (see Figure 6b) confirms that the different families can be distinguished by the duration between lunar encounters. As expected, these families are not conic trajectories, as large variations in lunar relative velocity can be observed due to solar perturbations, even for short flight times (see Figure 6a). The relative velocity of a conic solution would stay constant (dotted flat line in Figure 6a), which is clearly not the case here. The particular transfer solutions of interest that come back to the Moon at the low relative velocity (grey star markers in Figure 6a at the edge of each family) are plotted in Figure 7 for each family in the *xy* plane of the Earth-centered rotating frame (coordinate system that rotates with the Sun-Earth line). The lunar orbit is indicated with a lighter, red circle. Interestingly, there are striking similarities between the Foi solution and a Sun-Earth Distant Prograde Orbit (DPO) with apogees alter-

nately leading and trailing the Earth in its orbit about the Sun. For instance, one can check the trajectory of the WIND mission in 2000 that sent the spacecraft into a DPO for the first time.[17] Shadowing a DPO is not entirely surprising: according to dynamical system theory, periodic orbits are known to play a fundamental role in the motion flow of chaotic systems such as the three-body problem.[18] Table 4 and Table 5 give the chosen constants of the Sun-Earth CR3BP model and the parameters of the solutions, so that the trajectories shown in Figure 7 can be reproduced and used for other applications.

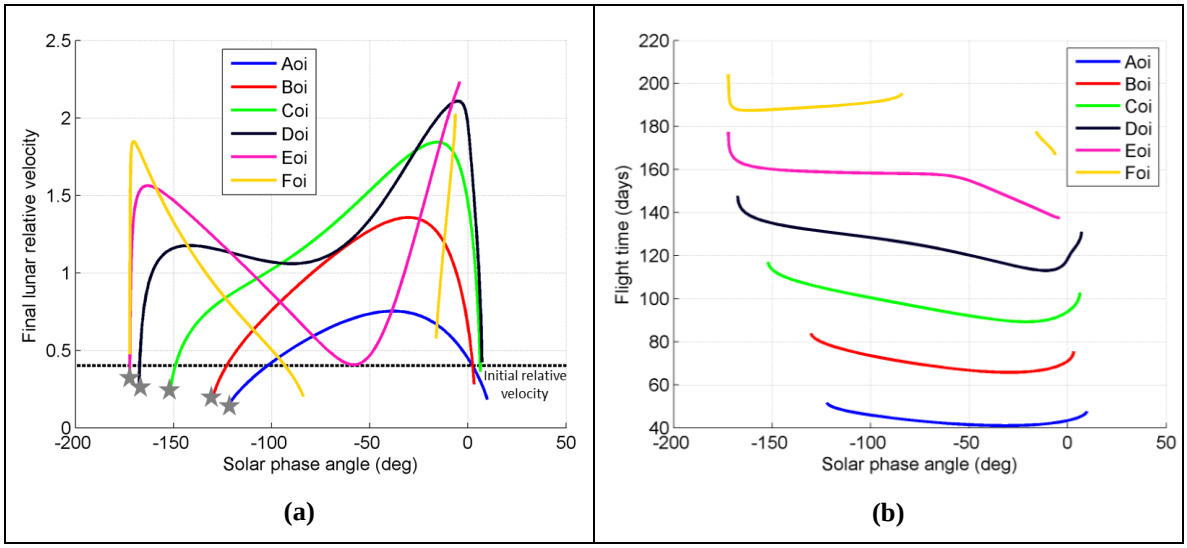

Figure 6. Characteristics of the 'oi' Moon-to-Moon families ($v_{\infty,0}$ = 0.4 km/s): (a) final lunar relative velocity magnitude vs solar phase angle (b) flight time vs solar phase angle.

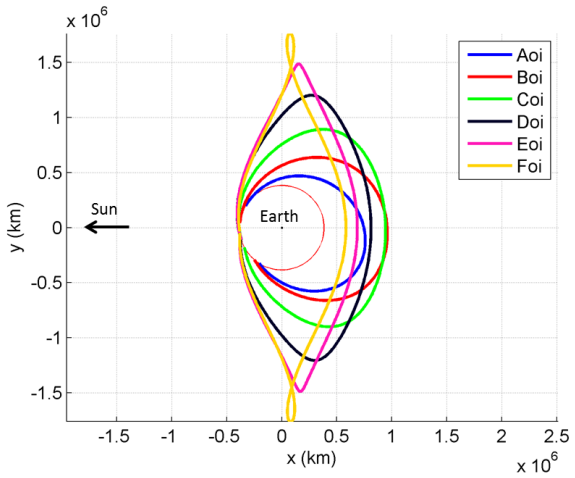

Figure 7. Moon-to-Moon 'oi' solutions with small lunar relative velocity on both ends, plotted in the Sun-Earth rotating frame.

All in all, the solutions shown in Figure 7 provide good initial guesses for transfers to/from the Moon with a low relative velocity. Thanks to simple database lookups, no a priori knowledge of the Sun-Earth CR3BP dynamics is necessary to find these solutions.

Table 4. Constants of the Sun-Earth-Moon model considered in the Moon-to-Moon phase.

Parameter	Value
Sun gravitational parameter	1.327124400419400e11 km2/s2
Earth gravitational parameter	3.986592936294783e5 km2/s2
Moon gravitational parameter	0 km2/s2 (massless)
Sun-Earth distance	150e6 km
Earth-Moon distance	3.844e5 km

Table 5. Transfer data of the family members plotted in Figure 7.

Family	$v_{\infty,0}$ (km/s)	θ_0 (deg)	α_0 (deg)	TOF (days)
Aoi	0.4	-122.2	80.5666	51.68
Boi	0.4	-130.3	73.0953	83.8407
Coi	0.4	-152.1	66.5158	116.9822
Doi	0.4	-167.6	57.8634	147.7553
Eoi	0.4	-172.3	48.9753	177.5771
Foi	0.4	-172.89	40.0815	206.1785

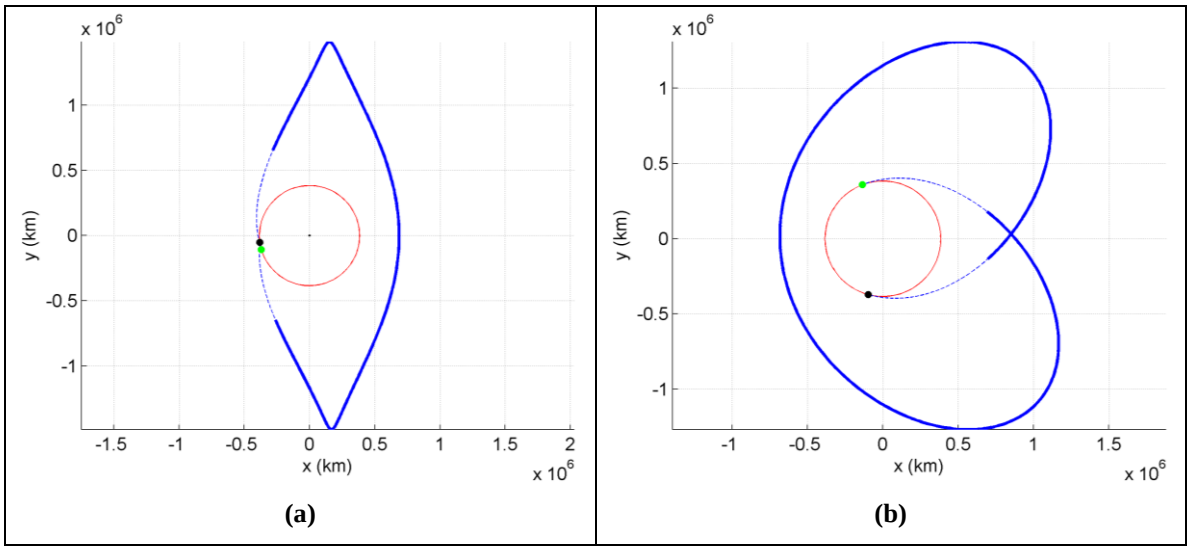

Figure 8. Selected Moon-to-Moon Eoi initial guess in: a) Earth-centered Sun-Earth rotating frame; b) Earth-centered inertial frame. The Moon's positions at the initial and final encounters are shown by black and green circles, respectively. Dashed lines are the chopped-off ends of the transfer that will be replaced by actual NRHO departure and DRO insertion trajectories.

Finally, the last step is to chop off both ends of the transfer below the chosen transition radius to the Moon (near 400,000 km in this analysis) that are dominated by the Moon's gravity. The initial guess strategies in these regions are different and described in the next two subsections. In

the rest of the paper, the Eoi Moon-to-Moon transfer is used to illustrate the methodology and construct a full initial guess. In a given month, the starting epoch is determined by the initial solar phase angle of -172.3 deg for this particular solution (see Table 5). Assuming a transfer scenario compatible with the ARRM timeline,[19] the lunar departure should happen around December 2027. The corresponding date with the appropriate solar phase angle is found to be December 26, 2027, which is the epoch assumed in the rest of this paper. The corresponding dates at the NRHO departure and DRO insertion interface points are January 04, 2028, and June 14, 2028, respectively. Figure 8 shows the Eoi initial guess for the Moon-to-Moon transfer phase in different frames.

DRO insertion

Next, an initial guess needs to be constructed for connecting the DRO orbit (described in the section about orbits considered) to the end of the Moon-to-Moon solution (described in the previous subsection) at the transition radius of 400,000 km. One common method of transferring to/from three-body orbits would be to use the unstable invariant manifolds of these orbits.[20] However, the selected DRO orbit is stable and therefore does not have unstable invariant manifolds. In addition, as explained at the beginning of this section, full ephemeris forces are considered in this phase and create a complex dynamical environment, so classical CR3BP theories cannot be used. Instead, a comprehensive numerical exploration of trajectories inserting into the DRO must be performed to fully understand the design space and select appropriate solutions.

To that end, the possible orbital motion of a spacecraft inserting into the DRO is simulated by applying a wide range of DV perturbations to the DRO nominal states and propagating backward in time the resultant states along a purely ballistic trajectory. A three-dimensional grid search samples three parameters:

- Flight time TOFi of the insertion phase: given the date at the interface point, the flight time value defines the time of insertion on the DRO, which then yields the insertion location on the DRO and the associated DRO nominal states. A range of TOFi values from 50 days to 100 days, in increments of 10 days, are considered.
- Planar components DVx and DVy of the DV perturbations at each impulse location, expressed in the Earth-Moon rotating frame, along the +x and +y directions, respectively. The x-axis points in the direction of the Moon's position vector with respect to the Earth, the z-axis is aligned with the angular momentum vector, while the y-axis completes the right-handed frame (approximately in the lunar velocity direction). Both perturbations are in the orbital plane of the Moon (perpendicular to the angular momentum vector of the Moon). DVy perturbation values are varied from -50 m/s to 50 m/s, with a 1 m/s step size. DVx perturbation values are varied from -25 m/s to 25 m/s, with a 0.001 m/s step size. This small step size is needed to yield a near exhaustive search considering the sensitivity of the trajectories, especially for long flight times. For simplicity, off-plane perturbations are not considered. Only one single impulse is used to reduce the dimensionality of the problem.

This grid results in 25 million points to be evaluated. Each point of the grid results in initial states that are numerically propagated backward over the flight time TOFi, using the JPL Planetary Ephemeris DE430 with gravitational point masses for the Sun, Earth, and the Moon (see Table 3). Using a multi-node cluster is recommended to propagate these trajectories in parallel and reduce the computation time. Trajectories are stored when their end states come within 200,000 km from the interface point states of the Moon-to-Moon transfer guess. These trajectories are then improved using a finer grid search around their initial states. Examples of possible DRO insertion trajectories found using this approach are shown in Figure 9-Figure 14. Table 6 provides the corresponding initial states used for each trajectory example.

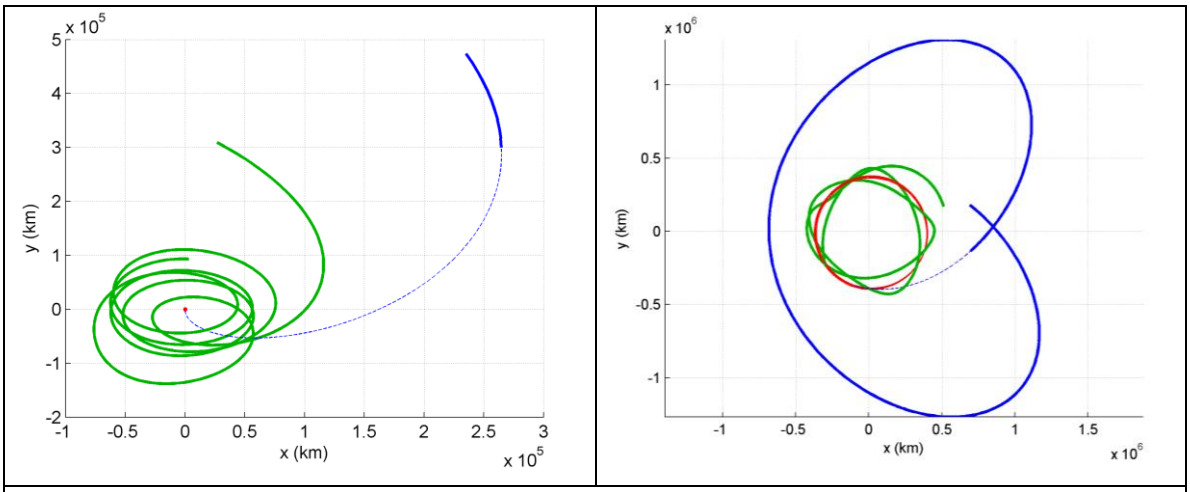

Figure 9. Example of DRO insertion trajectory (TOFi = 71.2 days, DVx = -16 m/s, DVy = 12.5 m/s). Left: Moon-centered Earth-Moon rotating frame. Right: Earth-centered inertial frame.

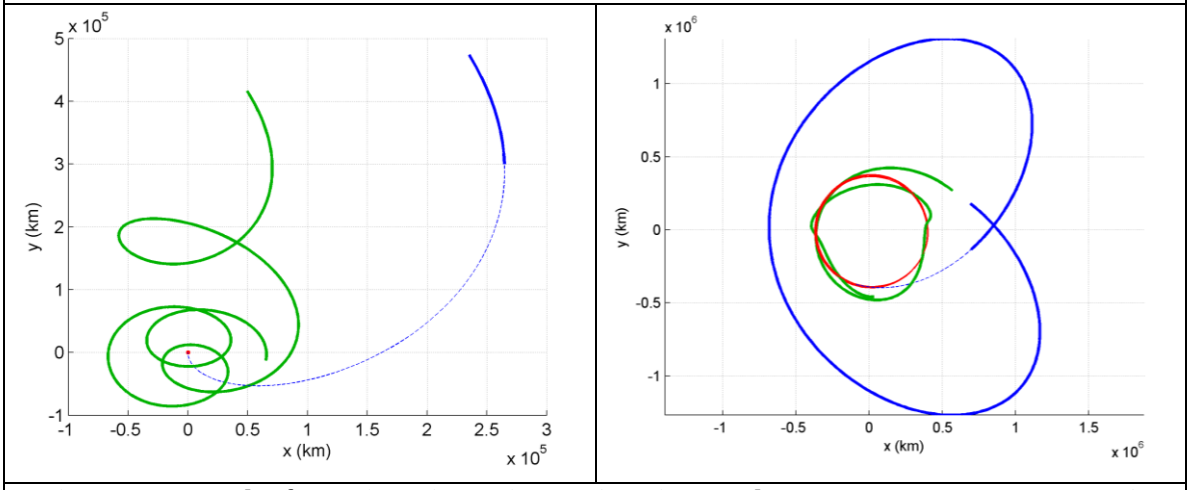

Figure 10. Example of DRO insertion trajectory (TOFi = 49.2 days, DVx = 21 m/s, DVy = 50 m/s). Left: Moon-centered Earth-Moon rotating frame. Right: Earth-centered inertial frame.

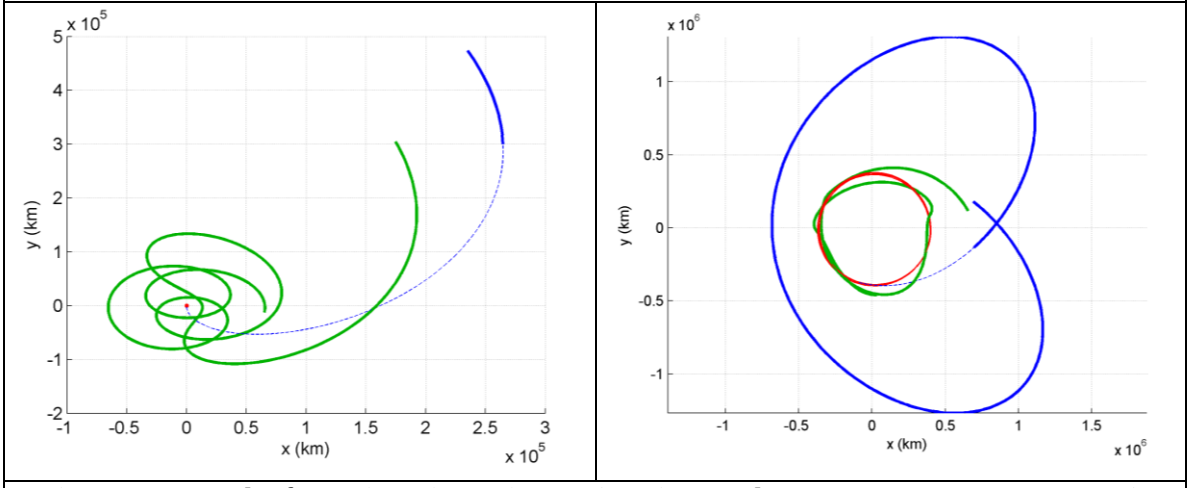

Figure 11. Example of DRO insertion trajectory (TOFi = 49.2 days, DVx = 25 m/s, DVy = 50 m/s). Left: Moon-centered Earth-Moon rotating frame. Right: Earth-centered inertial frame.

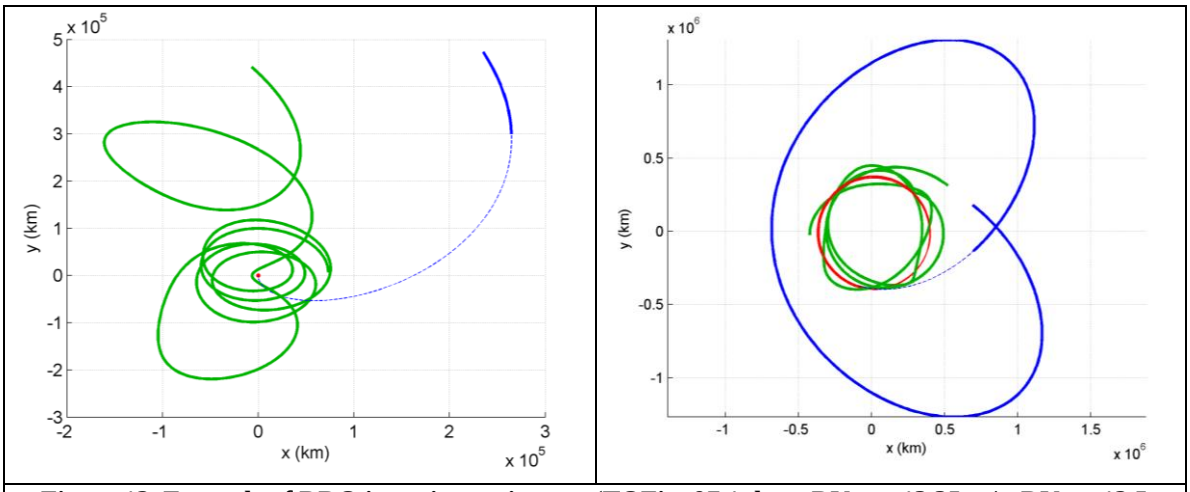

Figure 12. Example of DRO insertion trajectory (TOFi = 97.1 days, DVx = -13.35 m/s, DVy = 12.5 m/s). Left: Moon-centered Earth-Moon rotating frame. Right: Earth-centered inertial frame.

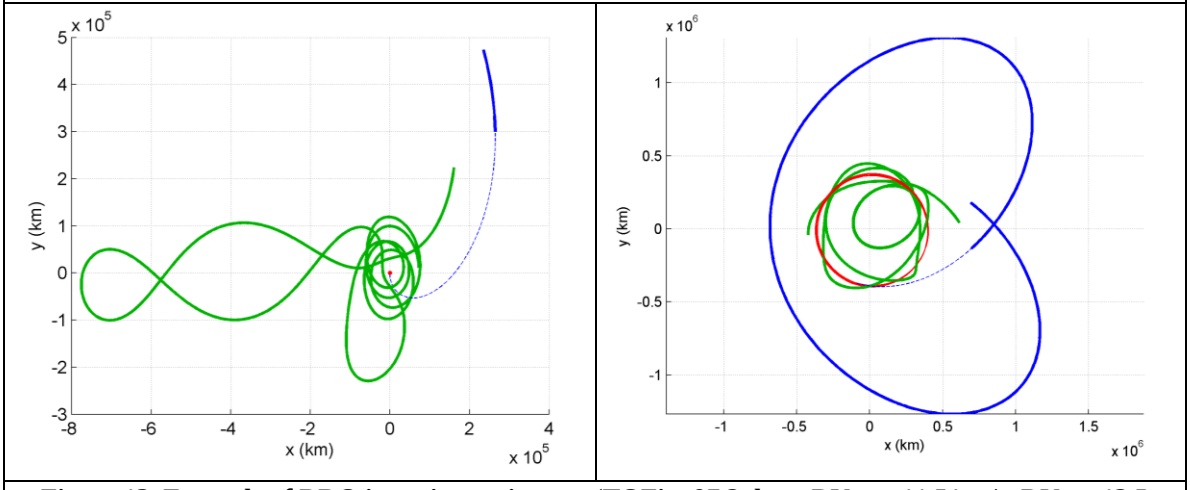

Figure 13. Example of DRO insertion trajectory (TOFi = 97.2 days, DVx = -11.51 m/s, DVy = 12.5 m/s). Left: Moon-centered Earth-Moon rotating frame. Right: Earth-centered inertial frame.

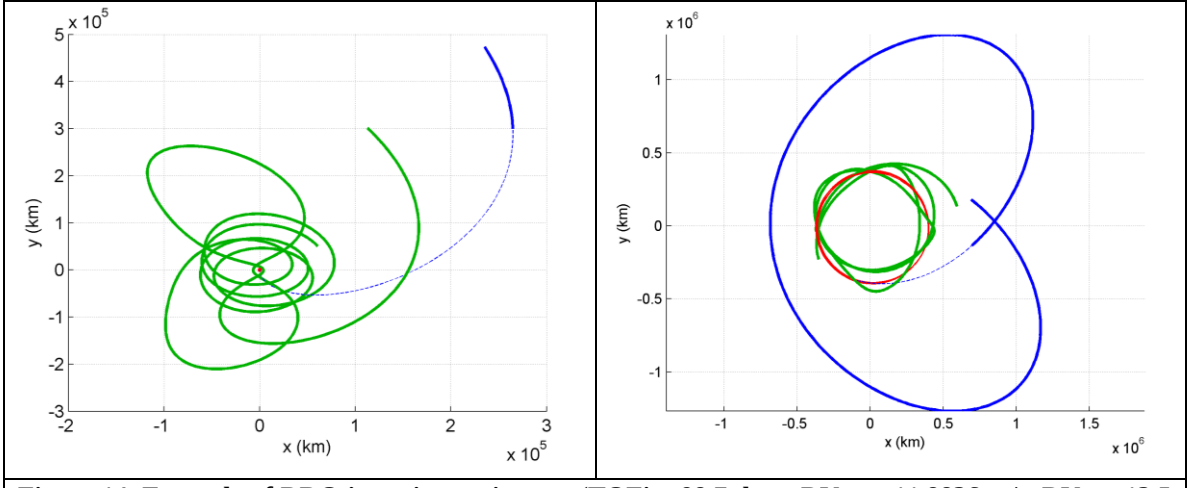

Figure 14. Example of DRO insertion trajectory (TOFi = 98.7 days, DVx = -11.8826 m/s, DVy = 12.5 m/s). Left: Moon-centered Earth-Moon rotating frame. Right: Earth-centered inertial frame.

Table 6. Initial DRO states for each DRO insertion scenario presented in Figure 9 - Figure 14, expressed in Earth-centered, EMO2000 frame.

Case	Figure 9	Figure 10	Figure 11	Figure 12	Figure 13	Figure 14
Epoch	2028 Aug 24 07:08:40.83	2028 Aug 02 07:08:40.83	2028 Aug 02 07:08:40.83	2028 Sep 19 04:44:40.83	2028 Sep 19 07:08:40.83	2028 Sep 20 19:08:40.83
x (10^5 km)	-2.94337215	0.32638621	0.32638621	-4.23232269	-4.21822834	-3.51070750
y (10^5 km)	-2.37471159	-4.58803915	-4.58803915	-0.25349158	-0.40582082	-2.30223128
z (10^5 km)	-0.32556280	-0.13738915	-0.13738915	-0.35384690	-0.35757743	-0.35956772
vx (km/s)	0.29654519	0.68540453	0.68540453	0.02780024	0.04044753	0.26225358
vy (km/s)	-1.01657680	0.05861099	0.05861099	-0.77832732	-0.77847814	-0.78304420
vz (km/s)	-0.01007638	0.06197382	0.06197382	-0.02032763	-0.01919375	0.00006428

One can observe an interesting topology of the trajectory space with different insertion 'families':

- Family with only retrograde close approaches of the Moon (see Figure 9). This is the most common solution.
- Family with a 1:1 loop with the Moon on the leading edge (see Figure 10). This trajectory type is similar to the DRO capture trajectories around Europa found by Lam.[21]
- Family with a prograde flyby on the far side of the Moon (see Figure 11).
- Family with a 1:1 loop and a prograde flyby on the near side of the Moon (see Figure 12).
- Family passing through an interior resonance with the Moon and a prograde flyby on the near side of the Moon (see Figure 13). In the particular example shown in Figure 13, the trajectory is close to be in 2:1 resonance with the Moon's orbital period at the beginning of the insertion phase.
- Family with two prograde flybys (alternately on the far side and on the near side of the Moon). Interestingly, the trajectory near the two prograde flybys looks similar to Earth-Moon DPOs (see Reference 22 for examples of lunar DPOs).

Similar families are observed for other DROs and/or different epochs. However, due to the sensitivity of these trajectories, it is hard to predict the initial conditions that will result in one trajectory type or another. It is therefore recommended to redo the grid search if a different DRO is used.

Although the DRO is inherently retrograde, it is interesting to note that many families arrive at the DRO after one or more prograde lunar flybys. This finding is in agreement with recent studies investigating trajectories approaching DROs.[23] These prograde flybys can be exploited to reduce the cost of the transfer (by changing some inclination for free for instance). The solution with two prograde flybys (see Figure 14) is therefore selected for the initial guess of the insertion phase.

Unsurprisingly, for each family, the insertion DV increases as the flight time decreases. DV perturbations as low as 15 m/s can produce feasible trajectories inserting into the DRO in 100 days, including 2 prograde flybys. Note that the delta-v values presented in Figure 9 – Figure 14 are not optimized. Less costly trajectories may be feasible, especially if other maneuvers are added. This limitation is not an issue as the initial guess trajectories are to be optimized (see Optimization section).

NRHO departure

The initial guess generation for the NRHO departure trajectory relies on the same concept as the one developed for the DRO insertion trajectory (see subsection above). A grid search is still used to vary flight time TOFd and initial impulse values. The resulting trajectories are propagated numerically forward in time, and only the solutions ending near the interface point are kept. Compared to the DRO insertion strategy, the main difference is that only one delta-v value (DVt) is considered, expressed along the instantaneous NRHO rotating velocity vector. This simple delta-v parameterization is more convenient because the NRHO orbit is not planar. It was found that the resulting solutions have significantly less topological variety than the DRO insertion solutions. Figure 15 shows an example of a NRHO departure trajectory found using this method.

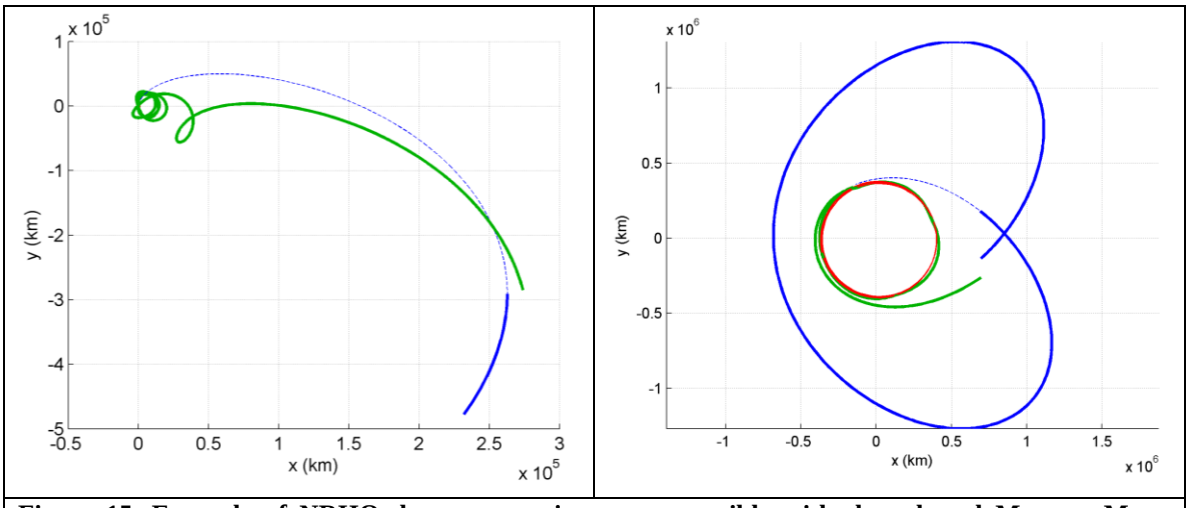

Figure 15. Example of NRHO departure trajectory compatible with the selected Moon-to-Moon transfer (TOFi = 98.7 days, DVx = -11.8826 m/s, DVy = 12.5 m/s). Left: Moon-centered Earth-Moon rotating frame. Right: Earth-centered inertial frame.

Table 7. Initial NRHO state for the NRHO departure scenario presented in Figure 15, expressed in Earth-centered, EMO2000 frame.

Epoch	2027 NOV 18 11:56:43.16932
x (km)	-1.544820896168345e+5
y (km)	3.411741862658243e+5
z (km)	-0.263896322746243e+5
vx (km/s)	-0.988814926038582
vy (km/s)	-0.373833469413345
vz (km/s)	-0.490192316409305

OPTIMIZATION & RESULTS

The resulting complete initial guess has discontinuities between each phase (see Figure 16). To enforce continuity and minimize delta-v, a local optimizer must be used to produce the final solution. In this analysis, the optimizer is based on the OPTIFOR framework.[24] In this frame-

work, the complete trajectory is broken down into different legs, which facilitates the modeling of continuity constraints between phases and reduces the extreme sensitivity of the dynamics near the Moon. The endpoints (states and times) of the transfer are fixed to ensure the desired orbits are used. Multiple impulsive maneuvers are distributed on each leg and can be varied by the optimizer. Despite being modeled as impulsive for simplicity, these maneuvers are typically small and can approximate well enough low-thrust arcs if needed. The resulting discrete problem is solved using SNOPT, a state-of-the-art non-linear programming solver.[25]

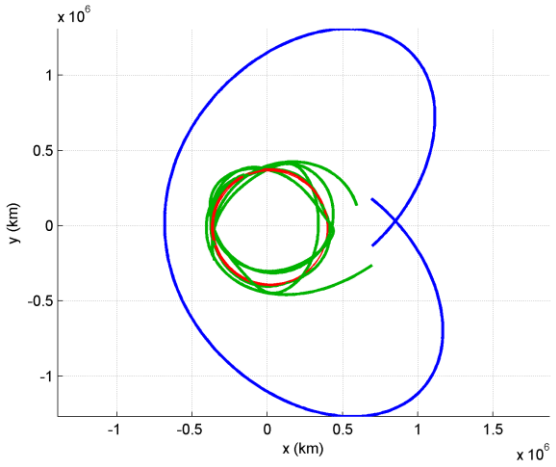

Figure 16. Complete initial guess of the NRHO to DRO transfer.

The converged solution is shown in Figure 17 – Figure 19. The overall structure of the initial guess was conserved, with the same number of revolutions around the Moon in the DRO insertion phase. Total ΔV is 56 m/s (NRO departure = 5 m/s, Solar Loop = 38 m/s, DRO insertion = 13 m/s). Note that this delta-v budget does not include statistical maneuvers. Flight time is ~11 months (336 days). There is only one 60-min lunar eclipse. Transfer starts on Nov 18, 2027, and ends on Oct 20, 2028.

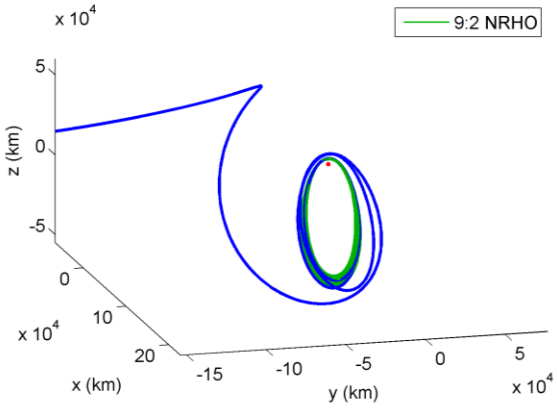

Figure 17. Optimized NRHO departure (lunar-centered Earth-Moon synodic frame).

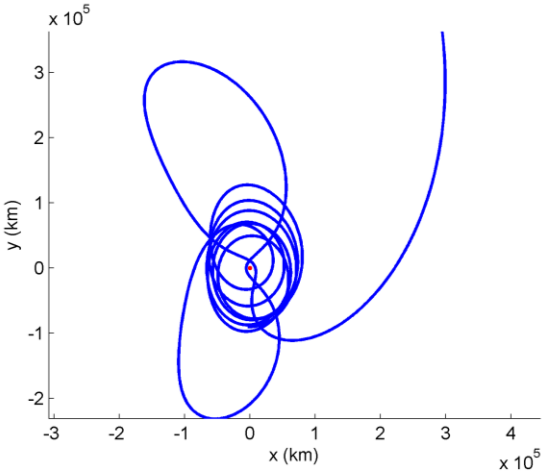

Figure 18. Optimized DRO insertion (lunar-centered Earth-Moon synodic frame).

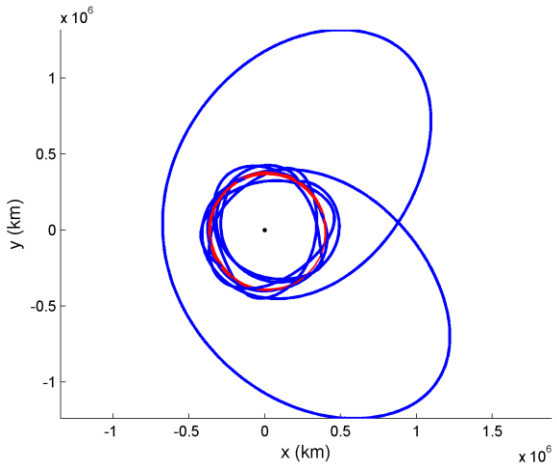

Figure 19. Optimized NRHO to DRO transfer (Earth-centered inertial frame).

The same approach was then applied when the Doi and Foi Moon-to-Moon transfers are used. Using similar DRO insertion and NRHO departure trajectories, the delta-v and flight time of the resulting transfers are given in Table 8. As expected, total delta-v is lower for longer flight times, since the spacecraft velocity is lower at larger distances from the Earth and the corresponding inclination change maneuver is reduced.

Table 8. Characteristics of NRHO to DRO transfers for different Moon-to-Moon families

Moon-to-Moon family	Total Delta-v	Total Flight time
Doi	85 m/s	306 days
Eoi	56 m/s	336 days
Foi	47 m/s	365 days

CONCLUSION

A systematic methodology to compute efficient NRHO to DRO transfers is described. Several transfer options and characteristics are identified, including different transfer durations and various DRO departure scenarios. In particular, two lunar prograde flybys on the near- and far-side of the Moon are found to be beneficial for inserting into DROs. This paper therefore provides a better understanding of the delta-v costs and flight times for efficient NRHO to DRO transfers. Nevertheless, the solutions found are not claimed to be globally optimal and further improvements are still possible in future work.

The methodology presented in this paper has the potential to facilitate the trajectory design for both robotic and manned missions in cislunar space. This methodology could be readily extended to other types of orbit transfers, such as transfers between DROs and any libration point orbits for instance.

ACKNOWLEDGMENTS

This research was carried out at the Jet Propulsion Laboratory, California Institute of Technology, under a contract with the National Aeronautics and Space Administration.

REFERENCES

[1] Whitley R., Martinez R., "Options for Staging Orbits in Cislunar Space," IEEE Aerospace 2015, Mar. 2015.

[2] Williams J., Lee D. E., Whitley R. L., Bokelmann K. A, Davis D. C., and Berry C. F., "Targeting Cislunar Near Rectilinear Halo Orbits for Human Space Exploration," No. AAS 17-267, Feb. 2017.

[3] Guzzetti D., Zimovan E., Howell K., and Davis D., "Stationkeeping Methodologies for Spacecraft in Lunar Near Rectilinear Halo Orbits," 27th AAS/AIAA Space Flight Mechanics Meeting, Feb. 2017.

[4] Bezrouk, C. J., Parker, J. S., "Long duration stability of Distant Retrograde Orbits," AIAA/AAS Astrodynamics Specialist Conference, No. AIAA 2014-4424, San Diego, California, 4-7 August 2014.

[5] Gates M., Muirhead B., Naasz B., McDonald M., Mazanek D., Stich S., Chodas P., Reuter J., "NASA's Asteroid Redirect Mission Concept Development Summary," presented at the IEEE Aerospace Conference, Big Sky, MT, 2015.

[6] Strange N., Landau L., McElrath T., Lantoine G., and Lam T., "Overview of Mission Design for NASA Asteroid Redirect Robotic Mission Concept" IEPC-2013-321 Presented at the 33rd International Electric Propulsion Conference The George Washington University Washington D.C. October 6-10 2013.

[7] Parrish, N. L., Parker, J. S., Hughes, S. P., Heiligers J., "Low-Thrust Transfers from Distant Retrograde Orbits to L2 Halo Orbits in the Earth-Moon System", International Conference on Astrodynamics Tools and Techniques (ICATT) 2016; 6th; 14-17 Mar. 2016; Darmstadt; Germany.

[8] Howell K., and Breakwell J., "Almost Rectilinear Halo Orbits,"Celestial Mechanics, Vol. 32, No. 1, 1984, pp. 29–52.

[9] Wilson R., Derivation of Differential Correctors Used in GENESIS Mission Design, Tech. Rep. JPL IOM 312.I-03-002, Jet Propulsion Laboratory, California Institute of Technology, 2003.

[10] Broucke R. A., "Periodic Orbits in the Restricted Three-Body Problem with Earth-Moon Masses," Tech. Rep. 32-1168, Jet Propulsion Laboratory, Cal. Tech., 1968.

[11] Henon, M., "Numerical Exploration of the Restricted Problem. VI. Hill's Case: Non-Periodic Orbits," Vol. 24, 1970, pp.24-31.

[12] Davis D. C., Bhatt S. A., Howell K. C., Jang J., Whitley R. L., Clark F. D., Guzzetti D., Zimovan E. M., and Barton G. H., "Orbit Maintenance and Navigation of Human Spacecraft at Cislunar Near Rectilinear Halo Orbits," 27th AAS/AIAA Space Flight Mechanics Meeting, Feb. 2017.

[13] Belbruno E. A., "Low energy method for changing the inclinations of orbiting satellites using weak stability boundaries and a computer process for implementing same," Patent US6253124B1, Jun 2001.

[14] Bate R. R, Mueller D. D., White J. E., Fundamentals of Astrodynamics, New York, Dover Publications. pp. 333–334, 1971.

[15] Parker J. S., Born G. H., "Modeling a low-energy ballistic lunar transfer using dynamical systems theory," Journal of Spacecraft and Rockets, Vol. 45, No. 6, 2008, pp. 1269–1281.

[16] Lantoine, G. and McElrath, Timothy P., "Families of Solar-Perturbed Moon-to-Moon Transfers", 24th AAS/AIAA Space Flight Mechanics Meeting, AAS 14-233, Santa Fe, New Mexico, January 26-30, 2014.

[17] Franz H., "WIND Lunar Backflip and Distant Prograde Orbit Implementation," AAS 01-173, AAS/AIAA Spaceflight Mechanics Meeting, Santa Barbara, California, USA, February 2001.

[18] Ott E., "Chaos in Dynamical Systems," 2nd ed. Cambridge University Press, Cambridge, 1993.

[19] Melissa L. McGuire, Nathan J. Strange, Laura M. Burke, Steven L. McCarty, Gregory B. Lantoine, Min Qu, Haijun Shen, David A. Smith, and Matthew A. Vavrina, "Overview of the Mission Design Reference Trajectory for NASA's Asteroid Redirect Robotic Mission (ARRM), AAS/AIAA Astrodynamics Specialist Conference, Columbia River Gorge, Stevenson, WA, August 20-24, 2017.

[20] Gómez G., Koon W. S., Marsden J. E., Masdemont J., and Ross S. D., "Connecting Orbits and Invariant Manifolds in the Spatial Restricted Three-Body Problem," Nonlinearity, Vol. 17, September 2004, pp. 1571–1606.

[21] Lam, T., Whiffen, G.J.: Exploration of Distant Retrograde Orbits Around Europa, Paper AAS05-110, Jan 2005.

[22] Mingotti, G., Topputo, F., Bernelli-Zazzera, F., "Transfers to distant periodic orbits around the Moon via their invariant manifolds," Acta Astronautica, Vol. 79, 2012, pp. 20–32.

[23] Kathryn E. Davis and Jeffrey S. Parker, "Prograde Lunar Flyby Trajectories From Distant Retrograde Orbits," AAS 15-775, 2016.

[24] Lantoine, G., "A Methodology for Robust Optimization of Low-Thrust Trajectories in Multi-Body Environments," Ph.D. Thesis, Georgia Institute of Technology, 2010.

[25] Gill P. E., Murray W., and Saunders M. A., "SNOPT: An SQP algorithm for large-scale constrained optimization", SIAM Journal on Optimization, 12:979-1006, 2002.